6^{th}GCSS WG-1 Intercomparison : ARM

A.R.Brown

31^{st}March 1999

1 Introduction

The last two GCSS working group 1 intercomparisons (BOMEX and ATEX) have studied cumulus in quasi-steady state over the sea. This year, it was decided to look at the development of shallow cumulus over land. The case is based on an idealization of observations made at the Southern Great Plains (SGP) ARM site on 21^{st}June 1997. On this day, cumulus clouds developed at the top of an initially clear convective boundary layer. The large-scale forcing was weak compared to the surface forcing.

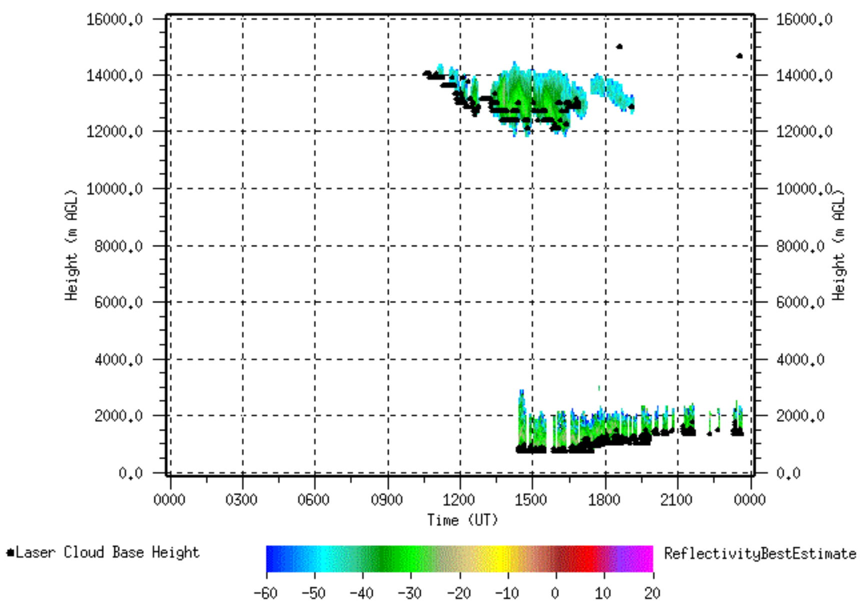

Figure 1: Radar reflectivity versus time at SGP central facility. Note formation of cumulus clouds at around 14.30 UTC (=8.30 local), gradually rising cloud base, and disappearance of last clouds at 23.30 UTC.

Some of the main issues that we would like the intercomparison to address are as follows:

- Do the models first produce cumulus clouds at approximately the correct time?
- Is there then a significant spin-up time for the cumulus circulations?
- Do the results for the cumulus layer (e.g entrainment rates, scalings) developed from the steadier over-sea cases still work well in this case?
- How is the subcloud layer affected by the developing cumulus? Do simple mixed layer scalings still work?

2 Setup Specifications

Note that when times are given in UTC they are in the form HH:MM e.g. 11.50 is eleven fifty (rather than half past eleven). However, for many purposes (e.g. specification of time-varying surface and large-scale forcings) it will be more convenient to use time given in seconds after 00.00 UTC on 21stJune.

The surface pressure should be set to 97000 Pa, and 100000 Pa should be used as the reference pressure for converting between potential temperature and temperature i.e.

$$T = \theta \left(\frac{P(z)}{100000} \right)^{R/C_p}$$

The following values for the constants should be used : $R = 287$ JK^{-1}Kg^{-1}, $C_p = 1004$ JK^{-1}Kg^{-1}, $g = 9.81$ ms^{-2}.

2.1 Initial Conditions

Figure 2 shows central facility sonde profiles of potential temperature (θ) and total water mixing ratio (q_t) at 11.30 UTC, 14.30 UTC, 17.30 UTC, 20.30 UTC and 23.30 UTC. At 11.30 UTC, there is a shallow

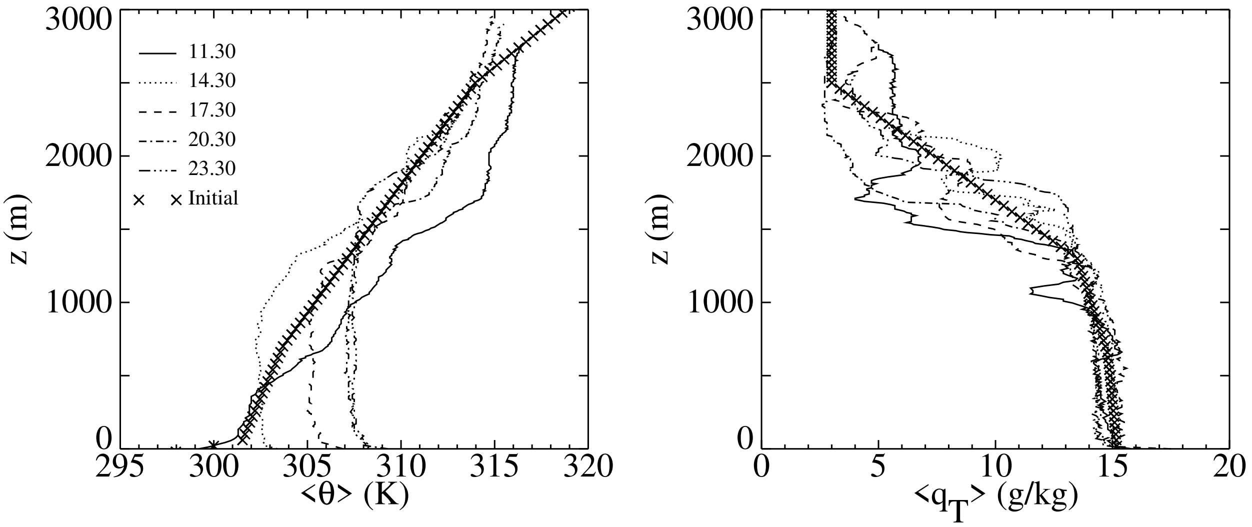

Figure 2: Central facility sonde profiles of θ and q_T. The crosses indicate the initial profiles to be used in the intercomparison.

stable boundary layer, but the inversion soon disappears once the surface heat flux becomes positive (around 12.30 UTC), and as expected, the boundary layer tends to warm and deepen through the day.

Given that the resolution used to allow use of a domain large enough to reasonably represent shallow cumulus convection will be far too coarse to explicitly resolve turbulence in the stable boundary layer, there seems little point in commencing the cloud resolving model simulations much before sunrise. Accordingly, it was decided to start at 11.30 UTC ($t = 41400$ s). The crosses on Figure 2 show the initial profiles to be used. Note that the initial temperature potential temperature profile is not closely matched to the observed profile. The reason for this is that the observations show a significant cooling from 500 m to 2000 m between 11.30 UTC and 14.30 UTC which is not provided by the diagnosed large-scale forcings. For this reason it seems sensible to start with a cooler profile than given by the observations. On the other hand, it is not desirable to start with a profile exactly like that observed at 14.30 UTC, as budget considerations suggest that the models could not then warm sufficiently to agree with the observations at later times. The chosen profile is therefore a compromise between the sonde profiles from 11.30 and

Table 1: Initial profiles of $\langle\theta\rangle$, $\langle q_T\rangle$, $\langle u\rangle$ and $\langle v\rangle$.

z (m)	$\langle\theta\rangle$ (K)	$\langle q_T\rangle$ (g/kg)	$\langle u\rangle$ (m/s)	$\langle v\rangle$ (m/s)
0.0	299.00	15.20	10.0	0.0
50.0	301.50	15.17	10.0	0.0
350.0	302.50	14.98	10.0	0.0
650.0	303.53	14.80	10.0	0.0
700.0	303.70	14.70	10.0	0.0
1300.0	307.13	13.50	10.0	0.0
2500.0	314.00	3.00	10.0	0.0
5500.0	343.20	3.00	10.0	0.0

14.30. Another minor modification that has been made is to slightly increase the potential temperature gradient above 2500 m in order to prevent any clouds from reaching the model's damping layer at 3500 m.

The initial potential temperature and total water content values to be used are given in Table 1. Linear interpolation should be used to obtain values at intermediate heights.

As well as ensuring that all models start with the same potential temperature profiles, it is important to ensure that they diagnose similar temperature profiles (as the diagnosed saturation mixing ratio depends strongly on temperature, changing by approximately 1 g/kg per degree at 700 m). For a quick check, my anelastic model gives $p = 89658$ Pa at 700 m, and $p = 72584$ Pa at 2500 m. This gives initial temperature values of 294.4 K and 286.5 K at these two heights. Please check that your values are close to these (e.g. within a few tenths of a degree at 700 m). Also, it is recommended that everybody uses the same saturation function, as suggested by Bjorn last year. Code for this is given below. Microphysics parametrizations should be switched off for the standard intercomparison run.

In the absence of detailed estimates of the time and height variation of the geostrophic wind, and of any large-scale advective tendencies of the wind components (see later), there seems to be little point in attempting to closely match the observed wind profiles. Accordingly, for simplicity, set the initial horizontal wind $(\langle u\rangle, \langle v\rangle)$ to (10,0) ms^{-1} at all levels, as indicated in Table 1.

Turbulence should be initiated by imposing random temperature perturbations, varying between ± 0.1 K at the surface. The magnitude of the perturbations should decrease linearly with height to zero at 200 m.

Models which carry a prognostic equation for subgrid TKE, should set subgrid TKE to $0.15 * (1.0 - z/150)$ for $z < 150$ m, and to zero for $z \geq 150$ m.

2.2 Fortran 90 code for saturation vapour mixing ratio calculation

```
c -----------------------------------------------------------------------
c This function calculates the saturation vapour mixing ratio for liquid
c water as a function of temperature and pressure, it is based on the
c polynomial fits of Flatau et al., (JAM 31:1507), it is written in F90
c
      real function rslf(p,t)

      implicit none
      real , intent(in)  :: p,t  ! pressure (Pa) Temperature (K)
      real                     :: x    ! a dummy variable

      real , parameter   :: eps=0.622,
     +      c0= .6105851e+03, c1= .4440316e+02, c2= .1430341e+01,
     +      c3= .2641412e-01, c4= .2995057e-03, c5= .2031998e-05,
     +      c6= .6936113e-08, c7= .2564861e-11, c8=-.3704404e-13
```

```
      x    = max(-80.,t-273.16)
      x    = c0+x*(c1+x*(c2+x*(c3+x*(c4+x*(c5+x*(c6+x*(c7+x*c8)))))))
      rslf = eps*x/(p-x)

      return
c
c ----------------------------------------------------------------------
```

2.3 Surface boundary condition

Figure 3 shows the surface energy balance for the SGP central facility on 21stJune. The strong diurnal

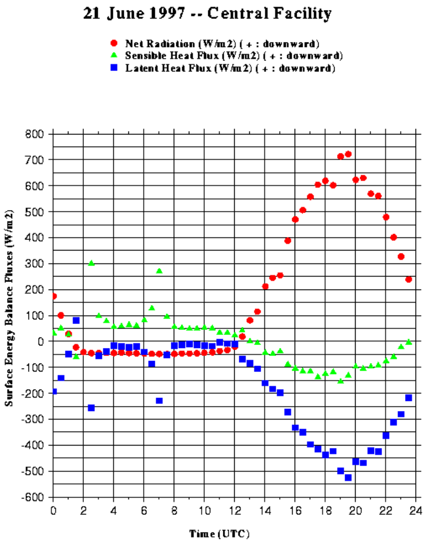

Figure 3: Surface energy balance at SGP central facility.

variation in the surface sensible and latent fluxes is clear. Note that the Bowen Ratios is around 0.3 for most of the day, compared to values of around 0.06 for the over-sea ATEX and BOMEX cases.

It has been decided that the surface scalar fluxes should be imposed in the intercomparison run. Table 2.3 gives values of the fluxes at a number of different times, and linear interpolation should be used to obtain the values to impose at intermediate times.

The surface roughness length should be set to 0.035 m (a characteristic value for the ARM site). Monin-Obukhov similarity can then be used to get the the friction velocity (u_*) at each surface point from the velocity at each of the lowest level interior points. If possible models should use $\phi_m = (1+4.8z/L)$ for stable conditions, and $\phi_m = (1 - 19.3z/L)^{-0.25}$ for unstable conditions. Code to get u_* for a given velocity and surface bouyancy flux is given below (thanks to Bjorn Stevens). It may be worth setting up a look-up table (as done in the UKMO model) in order to avoid having to iterate each time.

Table 2: Surface sensible (H) and latent (LE) heat fluxes to be imposed in model runs. Linear interpolation should be used to obtain the fluxes between the specified times. Please note that the specified times here are not the same as those used in specifying the large-scale forcing.

Time (s)	H (Wm^{-2})	LE (Wm^{-2})
41400	-30	5
55800	90	250
64800	140	450
68400	140	500
77400	100	420
86400	-10	180
93600	-10	0

```
! ----------------------------------------------------------------------
!
! DISCLAIMER : this code appears to be correct but has not been
!              very thouroughly tested. If you do notice any
!              anomalous behaviour then please contact Andy and/or
!              Bjorn
!
! Function diag_ustar:  returns value of ustar using the below
! similarity functions and a specified buoyancy flux (bflx) given in
! kinematic units
!
! phi_m (zeta > 0) =  (1 + am * zeta)
! phi_m (zeta < 0) =  (1 - bm * zeta)^(-1/4)
!
! where zeta = z/lmo and lmo = (theta_rev/g*vonk) * (ustar^2/tstar)
!
! Ref: Businger, 1973, Turbulent Transfer in the Atmospheric Surface
! Layer, in Workshop on Micormeteorology, pages 67-100.
!
! Code writen March, 1999 by Bjorn Stevens
!
! Code corrected 8th June 1999 (obukhov length was wrong way up,
! so now used as reciprocal of obukhov length)

      real function diag_ustar(z,bflx,wnd)

      implicit none
      real, parameter      :: vonk =  0.4   ! von Karmans constant
      real, parameter      :: g    = 9.81   ! gravitational acceleration
      real, parameter      :: z0   = 0.035  ! momentum roughness height
      real, parameter      :: am   =  4.8   !   "          "         "
      real, parameter      :: bm   = 19.3   !   "          "         "
      real, parameter      :: eps  = 1.e-10 ! non-zero, small number

      real, intent (in)    :: z             ! height where u locates
      real, intent (in)    :: bflx          ! surface buoyancy flux (m^2/s^3)
      real, intent (in)    :: wnd           ! wind speed at z

      integer :: iterate
      real    :: lnz, klnz, c1, x, psi1, zeta, rlmo, ustar

      lnz   = log(z/z0)
      klnz  = vonk/lnz
      c1    = 3.14159/2. - 3.*log(2.)
```

```
      ustar =  wnd*klnz
      if (bflx /= 0.0) then
        do iterate=1,4
          rlmo   = -bflx * vonk/(ustar**3 + eps)   !reciprocal of
                                                   !obukhov length
          zeta  = z*rlmo
          if (zeta > 0.) then
            ustar =  vonk*wnd  /(lnz + am*zeta)
          else
            x     = sqrt( sqrt( 1.0 - bm*zeta ) )
            psi1  = 2.*log(1.0+x) + log(1.0+x*x) - 2.*atan(x) + c1
            ustar = wnd*vonk/(lnz - psi1)
          end if
        end do
      end if

      diag_ustar = ustar

      return
      end function diag_ustar
! ----------------------------------------------------------------------
```

2.4 Large-scale forcing and radiation

Large-scale forcing terms have been estimated using a variational method (Zhang and Lin 1997) on observations from over the entire SGP site (an area of approximately 365 km by 300 km). Figure 4 shows the resulting combined large-scale horizontal and vertical advective tendency profiles for θ and q_t. The effects of both are small compared to the effects of the surface forcing (which is precisely why this case was chosen!). Accordingly, a very simple representation of these terms is appropriate (see below).

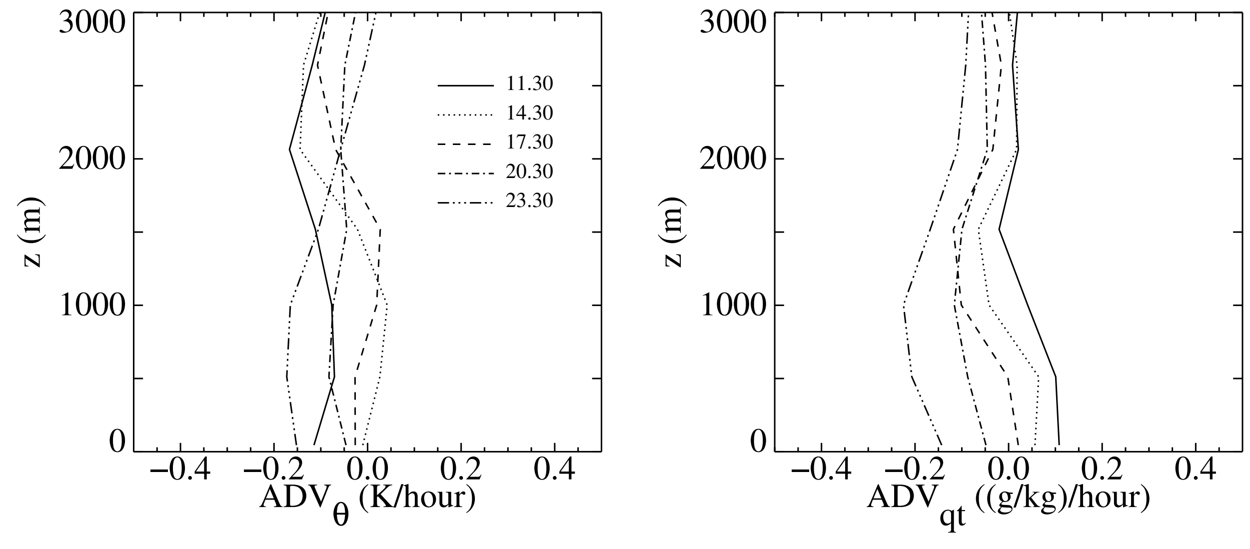

Figure 4: Diagnosed advective tendencies of θ and q_T at 11.30, 14.30, 17.30, 20.30 and 23.30 UTC.

Radiative tendencies have been estimated by running a simulation using an interactive two-stream radiation code (Edwards and Slingo, 1996). Figure 5 shows the diagnosed long wave (LW_θ), short wave (SW_θ) and total ($RAD_\theta = LW_\theta + SW_\theta$) heating rates from this simulation (averaged across the horizontal domain and over one hour). At 11.30 UTC, long wave cooling is almost unopposed by short wave warming, and so there is a net radiative cooling of the entire layer. However, at later times, there is an approximate balance between the long wave cooling and short wave heating, so that the averaged total radiative tendency is close to zero. The formation of clouds makes the profiles of LW_θ and SW_θ

Table 3: Magnitudes of large-scale advective forcing and radiative tendencies to be applied in lowest 1000 m *(note units!)*. Reduced tendencies are to be applied above 1000 m, as described in the text. Linear interpolation should be used to calculate forcings at intermediate times. Please note that the specified times here are not the same as those used in specifying the surface fluxes.

Time (s)	A_θ (K/hour)	R_θ (K/hour)	A_{qt} ((g/kg)/hour)
41400	0.000	-0.125	+0.080
52200	0.000	0.000	+0.020
63000	0.000	0.000	-0.040
73800	-0.080	0.000	-0.100
84600	-0.160	0.000	-0.160
93600	-0.160	-0.100	-0.300

less smooth (e.g. compare the 17.30 UTC profiles with those from 14.30 UTC) but the net averaged tendencies remain small. In principle, the effects of the much larger radiative tendencies that can occur within individual clouds might have a significant effect on them. However, tests in which the interactive radiation scheme was replaced with an imposition of a simple representation of this net averaged tendency gave very similar results (consistent with the earlier findings for shallow cumulus convection). Accordingly this simpler approach has been adopted for the present study.

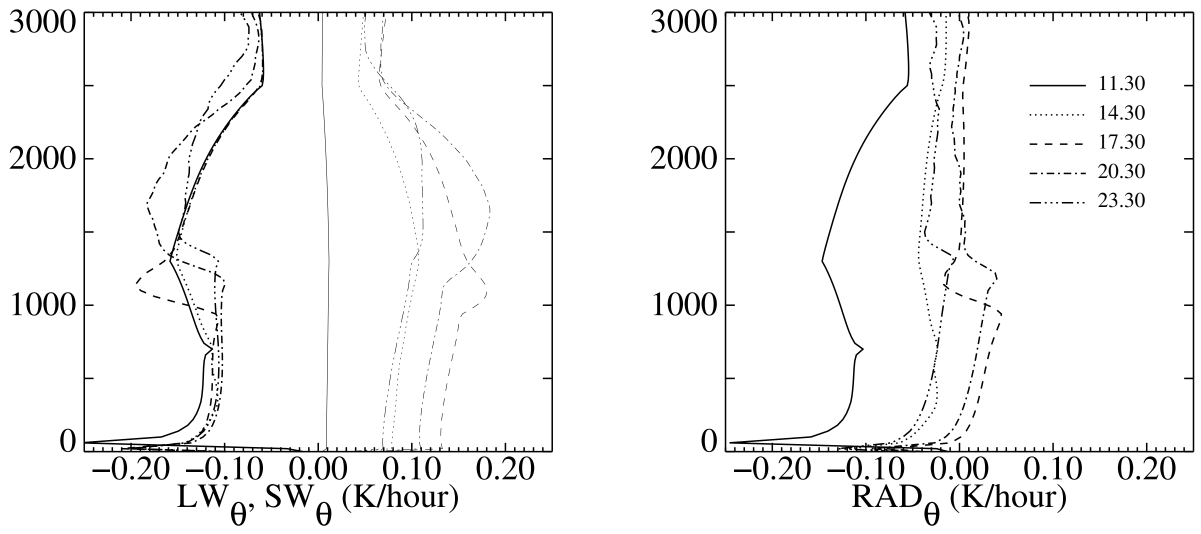

Figure 5: Diagnosed averaged radiative tendencies (LW_θ for long wave, SW_θ for short wave, and $RAD_\theta = LW_\theta + SW_\theta$ for total) from simulation using interactive radiation scheme.

Table 3 gives the values of A_θ, R_θ A_{qt} which are to be used to scale the values of the large-scale advective tendency of θ, of the large-scale advective tendency of q_t, and of the radiative tendency to be applied to θ. These values are given at various times, and linear interpolation should be be used to obtain values at intermediate times. Note that A_θ has been given a value of zero at 11.30 UTC to reflect the fact that the specified initial temperature profile is already colder than that from the sonde ascent at that time. Tendencies should then be applied to θ and q_t as follows.

For $z < 1000$ m,

$$\frac{\partial \theta}{\partial t} = ADV_\theta + RAD_\theta = A_\theta + R_\theta$$

$$\frac{\partial q_t}{\partial t} = ADV_{qt} = A_{qt}$$

For 1000 m $\leq z < 3000$ m,

$$\frac{\partial \theta}{\partial t} = ADV_\theta + RAD_\theta = (A_\theta + R_\theta)\,(1 - (z - 1000)/2000)$$

$$\frac{\partial q_t}{\partial t} = ADV_{qt} = A_{qt}\,(1 - (z - 1000)/2000)$$

and for $z \geq 3000$ m,

$$\frac{\partial \theta}{\partial t} = ADV_\theta + RAD_\theta = 0$$

$$\frac{\partial q_t}{\partial t} = ADV_{qt} = 0$$

No estimates of the geostrophic wind are presently available. Noting that the observed initial wind speeds above the boundary layer are approximately 10 ms^{-1}, it is proposed to set the geostrophic wind to (10,0) ms^{-1}. The Coriolis parameter should be set to 8.5×10^{-5} s^{-1}, as appropriate for a latitude of 36°N.

2.5 Numerical grid

The recommended domain size is 6400 m $\times$ 6400 m in the horizontal, with a depth of 4400 m. The vertical spacing should be 40 m, and ideally the horizontal spacing should be 66.67 m (96 points in each horizontal direction). If this is too expensive for anyone (the simulation is to be run for 14.5 hours), then results may be submitted using a horizontal resolution of 100 m (64 points in each direction). It is recommended that a damping layer is used above 3500 m.

3 Required output

The simulation is to be run from 11.30 UTC on June 21$^{\text{st}}$(t = 41400 s) until 02.00 UTC on June 22$^{\text{nd}}$(t = 93600 s).

Data is required as follows:

- Set A at the initial time
- Set G (time series) for the duration of the integration with a recommended 5 minute sample period
- All time averaged sets (A-F) for each full hour i.e.
  12.00 UTC ($t = 43200\ s$) to 13.00 UTC ($t = 46800\ s$),
  13.00 UTC ($t = 46800\ s$) to 14.00 UTC ($t = 50400\ s$),
  and so on, until
  01.00 UTC ($t = 90000\ s$) to 02.00 UTC ($t = 936000\ s$).

Results should be provided in ASCII format. At the top of each set should be a one line header indicating the set which follows, the time the calculations correspond to (take the middle point of one hour averages), the name of the participant and any other relevant information. For example:

'20.30 UTC E Andy 3D Run'

would be the header file for my set E averaged from 20.00 UTC until 21.00 UTC. Each row of numbers should be written in the format, ('99E15.7'). Datasets should be emailed to me at 'arbrown@meto.gov.uk'. (if email becomes a problem we will use anonymous ftp).